Nanoscale

Self-assembly of clay nanotubes on hair surface for medical and cosmetic formulations

Journal:	*Nanoscale*
Manuscript ID	NR-ART-07-2018-005949.R1
Article Type:	Paper
Date Submitted by the Author:	06-Aug-2018

Complete List of Authors:	Panchal, Abhishek; Louisiana Tech University, Institute for Micromanufacturing Fakhrullina, Gölnur; Kazanskij federal'nyj universitet, Institute of Fundamental Medicine and Biology Fakhrullin, Rawil; Kazanskij federal'nyj universitet, Institute of Fundamental Medicine and Biology; Louisiana Tech University, Institute for Micromanufacturing Lvov, Yuri; Louisiana Tech University, Institute for Micromanufacturing

Self-assembly of clay nanotubes on hair surface for medical and cosmetic formulations

*Abhishek Panchal, Gölnur Fakhrullina, Rawil Fakhrullin, Yuri Lvov**

Abhishek Panchal, Prof. Rawil Fakhrullin, Prof. Yuri Lvov
911 Hergot Avenue, Ruston, LA 71272, United States of America.
E-mail: ylvov@latech.edu
Gölnur Fakhrullina, Prof. Rawil Fakhrullin
Institute of Fundamental Medicine and Biology, Kazan Federal University, Kreml uramı 18, Kazan, Republic of Tatarstan, 420008, Russian Federation

Abstract: While most hair care formulations are developed on the basis of surfactants or polymers, we introduce self-assembly coating of micro and nano-particles as the underlying principle for hair modification, protection and enhancement. Halloysite clay nanotubes formed by rolled sheets of aluminosilicate kaolin assemble on the surface of hair forming a robust multilayer coverage. Prior to the application, clay nanotubes were loaded with selected dyes or drug allowing for hair coloring or medical treatment. This facile process is based on a 3-minute application of 1 wt. % aqueous dispersion of color/drug loaded halloysite resulting in ca. 3 μm thick uniform hair surface coating. This technique, which employs a very safe, biocompatible and inexpensive material, is ubiquitous with respect to species of source of hair and additives in solvent, making it viable as an excipient for conventional medical and veterinarian formulations.

1. Introduction

Hair, protein filaments covering the skin of mammals, including humans, plays a pivotal role in skin protection, thermoregulation and touch sensing. Decayed, damaged and depigmented (grey) hair is one of the most prominent indicators of disease and ageing. Although human hair loss is not fatal, it may affect mental well-being and requires medical intervention, including drug therapy.[1,2] Being one of the most visible human features, formulations augmenting the physical appearance of hair such as pigmentation have always been popular. Depending upon permanent or temporary color change, hair color products are formulated in many ways with different ingredients. Permanent (shampoo-resistant) hair dyes consist of color precursors which are oxidized on the hair surface by hydrogen peroxide. Contrary to damaging redox reactions, natural hair colors that have

been used for thousand years and are proven to be harmless.[3,4] However, formulating them into user-friendly products is a challenge: we have to trade-off convenient aqueous based application for cumbersome but longer lasting powder-based processes. Combining our experience with loading drug, dyes and polymer into the hollow lumen of clay nanotubes with self-assembly coating, we developed halloysites as micro-containers for efficient hair coloring.

To demonstrate the applicability of this technique to other facets of haircare, we have proposed anti-lice formulations with halloysite nanotubes. Hair in mammals may be affected by numerous diseases or infested by parasites. Fungal diseases, mites, lice and fleas depend on hair serving as a shelter and breeding habitat. Though parasites as lice are less common in developed nations, they are still posing a significant threat in developing countries, affecting millions.[5,6] The increased resistance of parasites due to ineffective delivery of anti-lice agents to hair surface warrants a better therapeutic system to treat infections on hair.[7]

Haircare formulation design often revolves around the intricate chemical and physical makeup of hair. For our technique, we highlight the importance of external surface of hair; especially microstructures which look like attached flakes with narrow gaps called cuticles (Figure 1A).[2] The cuticles - cortex composite structure serve as binding sites for targeted interactions to adsorb drugs or dye. Lasting hair treatments like conditioners are focused at surface binding driven by charge or applied to the inter-cuticle spaces, for enhanced absorption into the cortex.[5,6] Such formulations often disturb the natural chemistry of hair, causing their dryness, oxidation and discoloration.[6]

We employ halloysite clay nanotubes as a coating on hair via physical adsorption and self-assembly not involving any additional chemical treatment. In our approach toward both cosmetic and medical hair treatment, encasing of dyes and drugs in biocompatible halloysite clay followed by spontaneous self-assembly of these nanotubes on hair surface has been developed (Scheme 1). We fulfill two tasks: first encapsulating dye/drug into nanotubes, which allow usage of many different

compounds including those that are non-water soluble; and, second, assembling these loaded clay tubules onto hair surface.

Halloysite nanotubes (rolled kaolin sheets) are natural biocompatible clay available in large amounts at a low price.[8–13] Halloysite tubes have 50 - 60 nm external and 10 - 15 nm inner diameters with length within 0.5 - 1.5 μm.[8,14] Their walls are formed by the rolling of ca. 20 aluminosilicate layers.[8] The outer / inner surface chemistry of halloysite is remarkable: the external surface is composed of Si−O−Si groups, whereas the internal lumen surface consists of a gibbsite-like array of Al−OH groups.[8] Considering the positive / negative charges of alumina and silica substrates at pH 6.5, the ζ-potential of -30 mV was interpreted based on this charge separation.[15,16] These characteristics make halloysite nanotubes excellent vehicles for carrying numerous types of cargo (drugs, proteins, dyes, chemical inhibitors, metal nanoparticles), negatively charged materials are sucked into the tubes' lumens and positive ones adsorbed on the tubes' outer surfaces.[8,10,14,17–19] The typical halloysite loading mechanisms for negative or neutral molecules are driven by electrostatic interactions or precipitation from saturated solution into the lumen.[20,21] Diluted aqueous dispersions of halloysite (0.5 wt. %) stay suspended in water (pH 6.5) for 2-3 hours, and in the loaded state these nanotube colloids are stable for months.[8,22]

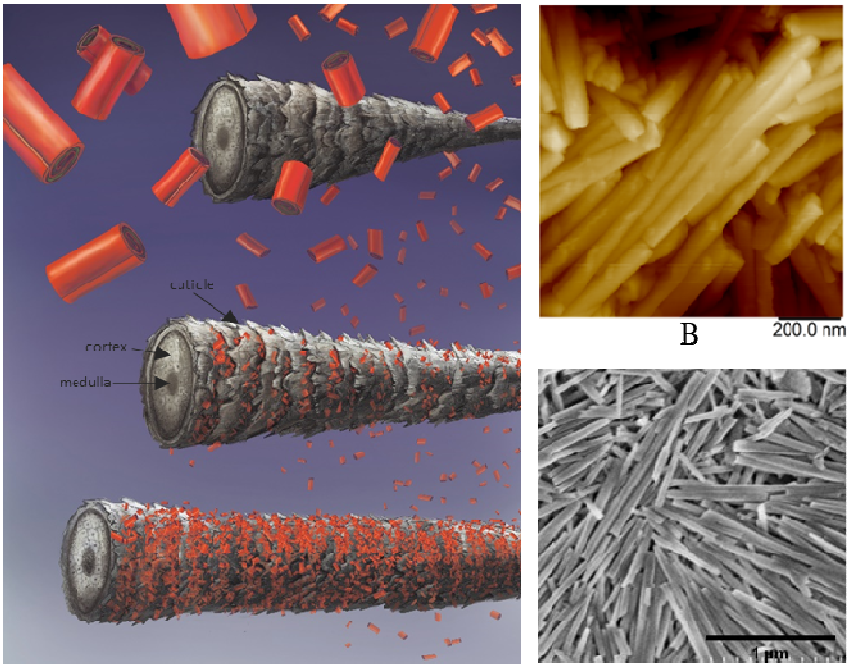

Scheme 1. Introduction to self-assembly of halloysite clay nanotubes on hair: Hair with applied clay nanotubes and development of the coating from anchoring in the cuticle to capillary force / drying driven surface assembly (A) and Atomic Force Microscopy (AFM) and Scanning Electron Microscopy (SEM) images of a group of dried clay nanotubes (B-C).

This allows for hydrophilic payloads and after the lumen hydrophobization, also for water-insoluble compounds, making these designed clay nanocapsules highly generic.[23] Such active core-shell tubule nanocapsules have been incorporated into different polymers to produce novel composites with tailored release profiles of active ingredients and to significantly extend their working duration (to weeks, and even months).[8,12,13,15] Many applications of halloysite as a container depend on loading capacity and its lumen diameter. Clay nanotubes with an enlarged cavity were prepared by a selective etching of alumina by its dissolution with acidic treatment. The halloysite etched with sulfuric acid, showed a four-time increase of loading capacity, from 9 to 35 wt. %.[13]

The strategy, illustrated here with hair colorants and insecticide drugs, is ubiquitous and can be extended to other medical hair treatments. Self-assembled nanoscale materials, including biomedical materials, depend on spontaneous assembly of nanosized elements into films, filaments, tubes or more complicated forms, eventually bound to a specific surface.[24–26] In clay-hair surface engineering, the assembly of the nanotubes in a multilayer coating is initiated in the hair cuticle

developing into a thicker layer during drying. This clay coating remains stable after shampoo and assumingly is stabilized by inter-tube Van der Waals attractive forces. One can control the density and thickness of the clay layers on hair by optimizing the suspension concentration, pH and halloysite hydrophobicity. The method works well on grey and pigmented human hair; animal hairs were also successfully coated (Figures S9-S11). A stable 3-5 μm thick coating using halloysite loaded with hair colorants or anti-lice drugs was achieved (Scheme 1). Surface-engineered hair clay coating is extremely resilient, enduring numerous washes.

We demonstrate the effective brown color restoration in grey hair and color change in young blond hair after their surface coating with the pigment-loaded halloysite nanotubes. Additionally, we have shown the proof-of-concept study on loading of drugs into the nanotubes with subsequent deposition onto hair. The clay nanotubes provide the extended release of drug onto hair and skin. Permethrin, a drug used in treatment of lice and scabies in humans and animals, was used as a model insecticide.[27,28] We have evaluated the drug release and insecticidal effects with *Caenorhabditis elegans* (free-living nematodes) resulting in efficient, long lasting suppression of their proliferation. This approach allows us to reduce the concentrations of insecticide drugs, thus minimizing the environmental pressure on useful insects like bees. It is useful for production of stable water-resistant drug-loaded clay hair coatings for medical and veterinary care, and for sustained nanoformulation of topical drugs, targeting fungal or autoimmune diseases, such as psoriasis.

2. Results and discussion

2.1 The halloysite assembly process.

Halloysite clay nanotubes form 2 hour stable aqueous dispersion at concentration 0.5-1 wt. %, rescinding with time to a denser very stable colloid at ca. 6 wt. % of clay in mixture.[15,23] Upon the minutes washing hair with 0.75 wt. % dispersion of pristine halloysite in water, pH 6.5 the surface of hair was covered with a layer of these clay nanotubes as shown in Figure 1 B, D. We believe

that drying is necessary final step fixing together the nanotube arrays. The EDX aluminium and silicon maps of alumina-silicate halloysite clay covered hair correspond to the deposits visible on the surface of hair (Figure 2).

The external covered surface of hair and the increased roughness indicates arrangement of halloysite only on the external surface. The coating is initiated from beneath the cuticles and spread along the flat surface (Figure 2). The deposits of clay tubes within inter-cuticle spaces were confirmed by TEM studies of cross-sections of halloysite coated human hair (Supplementary information-figure S2). Hair has a tendency to swell when wetted with water and its cuticles open up creating space for the dispersed halloysite to penetrate into it.[29–31] After drying, the cuticles close down to their initial state, trapping the tube arrays between them. This is evident in Figure 3 where tubes started anchoring at the inter-cuticle places and then spill out onto the surface of the adjoining cuticle (Figure 3) shows development of the halloysite nanoassembly with time from 0.5 to 3 min.

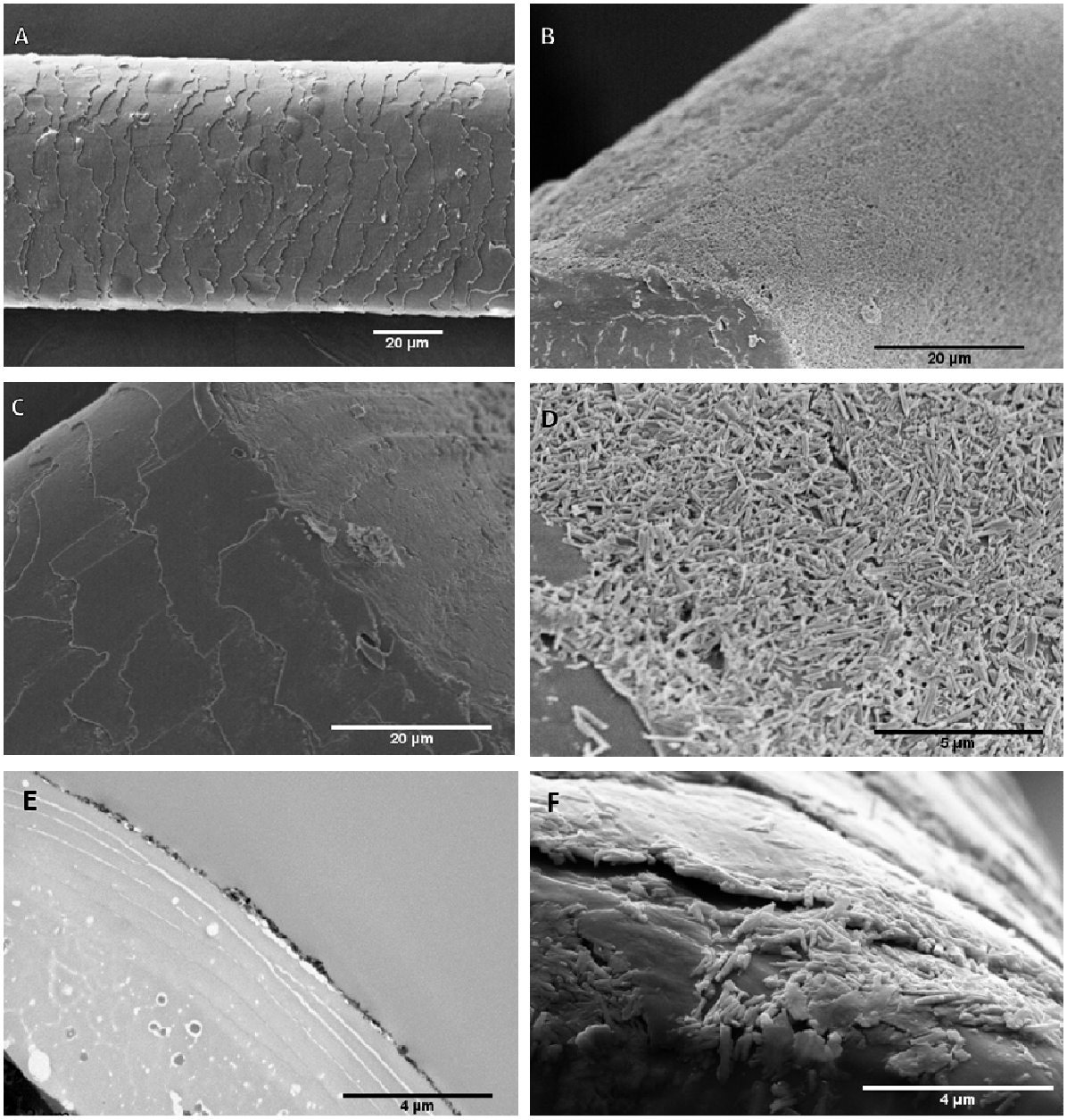

Figure 1: Self-assembly of halloysite clay nanotubes on hair surface: SEM images of pristine surface of human hair (A, C), and hair completely covered with halloysite nanotubes (B, D). The cross-section TEM image of coated with darker halloysite visible at the edge (E) and SEM of the same area (F).

The coating thickness is 3-5 µm and contains few layers of randomly attached clay nanotubes. The approximate quantitative evaluation of coating was done by combining optical (confocal) and electron microscopy results (TEM & SEM). The cross-section TEM image (Figure 1 E) provides with the thickness of the coating which is assumed to be spread over the curved surface area of a hair strand which is evaluated from the 3-D confocal & SEM images (Figure 1 A-C). The intrinsic

density of halloysite give you the approximate weight coating (1% by weight) and can be corroborated by TGA.

The nanotube coating on hair results in increase of the surface roughness of the hair by 30 - 50 % (Figure S1).

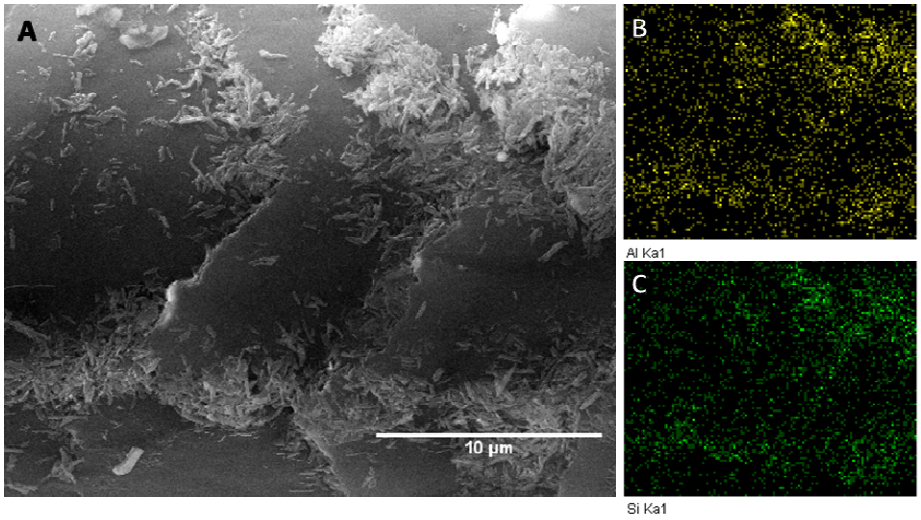

Figure 2. EDX mapping of halloysite on hair: aluminium (B) and silica (C) mapped images of hair coated with halloysite (A). Al and Si areas represent a distribution pattern of the aluminosilicate nanotubes on the hair surface. The detailed weight and atomic percentages are provided in Table S1.

Figure 3 reveals the cuticles of hair as anchoring sites for initiation of the nanotube self-assembly. One can see the progression of coating from pristine "bare" hair (B) to deposits from beneath the cuticles spreading to increasing amount of halloysite in their vicinity with longer time of dispersion exposure (C-D).

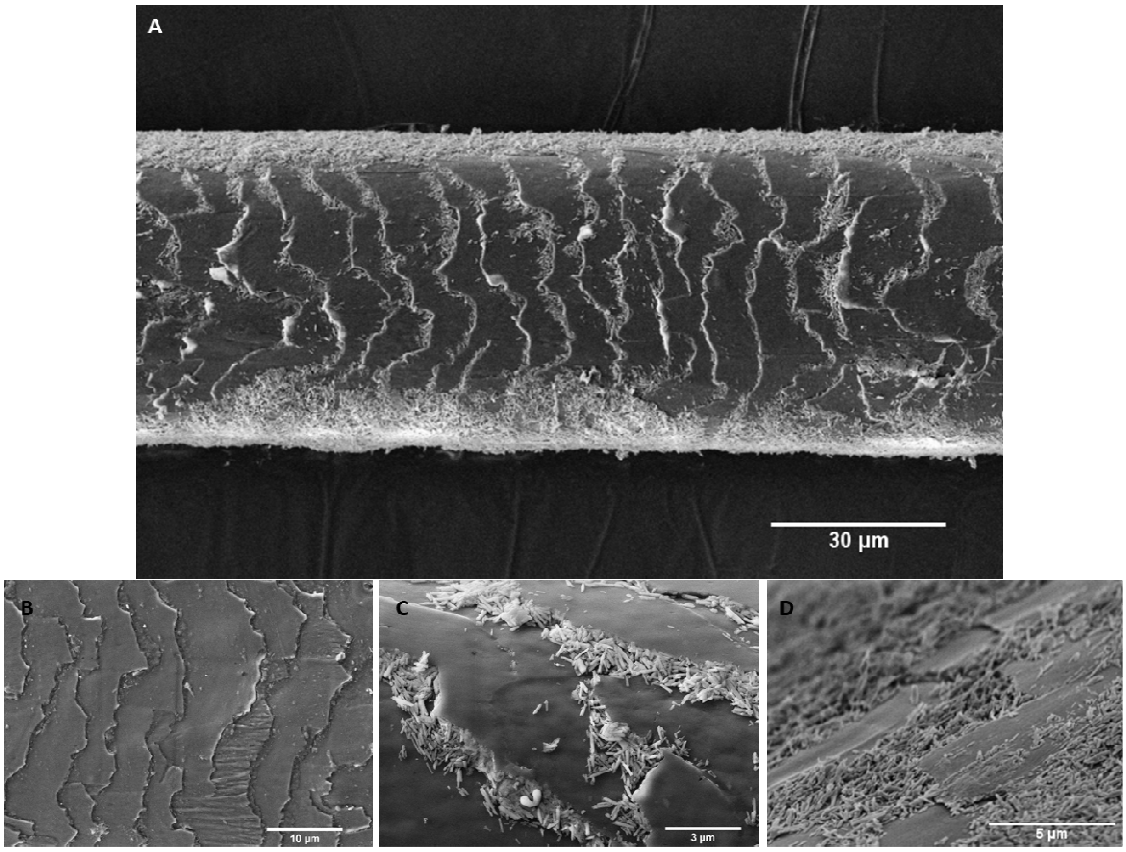

Figure 3. Development of nanotubes assembly with time: Partial coating of halloysite on hair (A) as a function of treatment time at 1, 2 and 3 mins (B-D) respectively.

2.1.1 Robustness of halloysite coating

The halloysite coating displayed robustness when subjected to a series of washings. To underline the strength of the coating, a strand of coated hair was washed in swirling water for one hour and then was examined under a 3-D confocal microscope (Figure 4). The halloysite coating analysed both visually and through roughness measurements, has shown good resistance to washing (the roughness characteristic for halloysite coating was reduced only by a small amount, Figure 4). Excluding any covalent bonds between the halloysite surface and the hair surface, hydrogen bonds and Van der Waals force tube-tube interactions remain as the possible reasons for this strong halloysite coating.

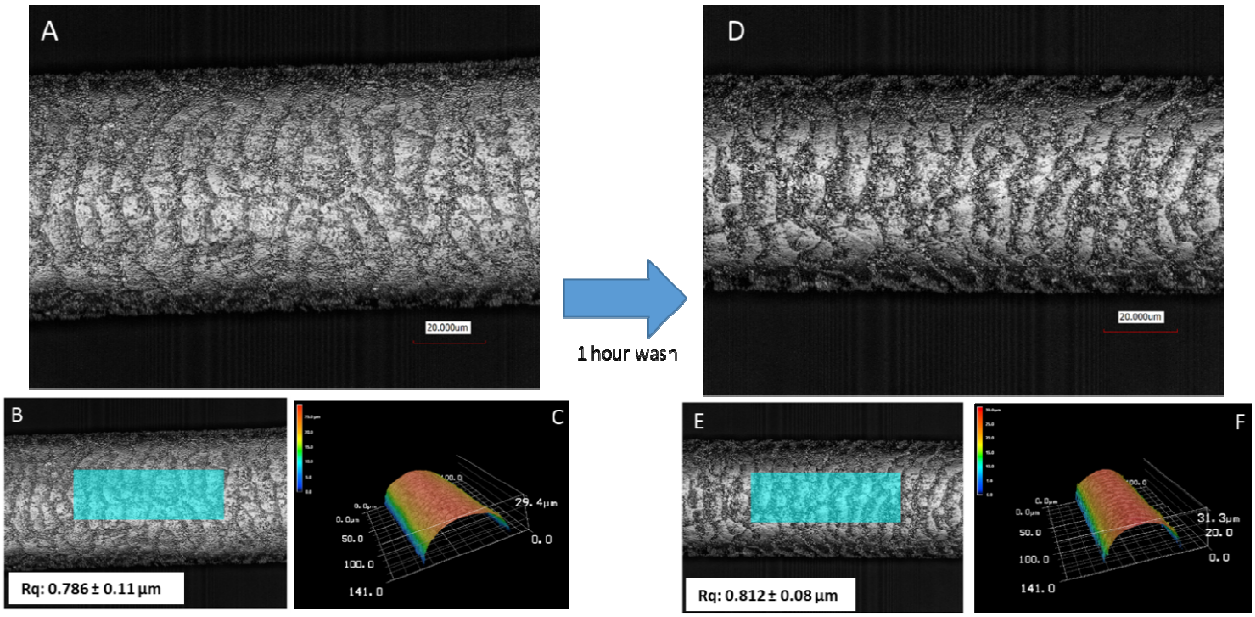

Figure 4: Robust clay coating: Images of surface of halloysite coated hair, before (A-C) and after (D-F) 1-hour shampoo wash, showing an intact layer of tubes on the surface and no significant change in surface roughness (Root mean square (Rq) values inset). Similar results have been obtained for coating with hydrophobised halloysite (Figures S4, S5)

Halloysite coating on hair is only on surface, and not embedded into the proteinaceous network of hair to affect any bulk mechanical properties (viz. elasticity and swelling). Being a surface coating, roughness is a mechanical property that can be affected and it has been shown to remain unchanged with coating

2.1.2 Hydrophobic halloysite interactions

Halloysites' external surface is composed of Si-OH groups which contribute to the dispersibility in water and the hydrogen bond-forming capacity of the nanotubes.[8] We modified halloysite surface to study possible change in the self-assembly process and to sort out type of forces involved. In order to render the halloysite hydrophobic, silane molecules with long aliphatic chains have been grafted on the Si-OH groups on the tubes' external surface.[28] The binding or adhesion of such tubes is predominantly due to Van der Waals forces as the hydroxyl centres contributing to hydrogen bonds have been shielded by the aliphatic group. The absence of hydrogen bonding groups on the surface make these tubes less stable in an aqueous dispersion favouring to the assembly on hair. The better assembly of hydrophobic halloysite on hair indicate the larger role that Van der Waals forces play in attaching tubes to hair surface (Figure 5).

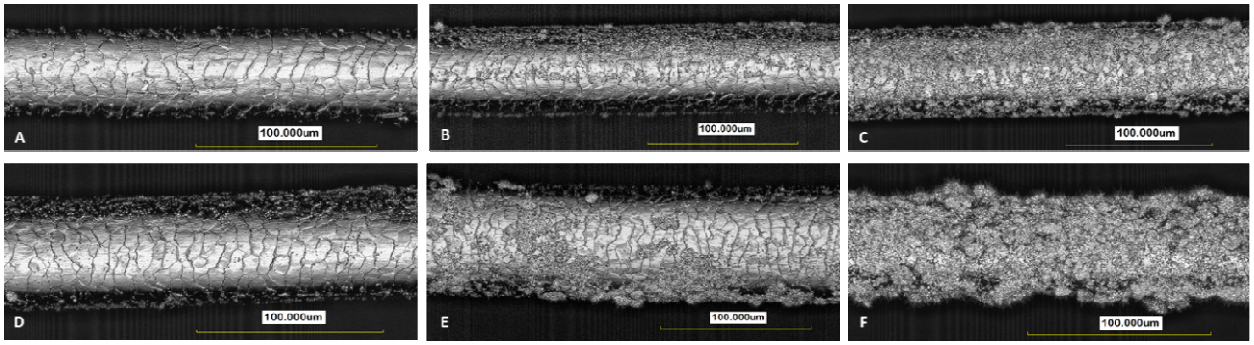

Figure 5. Coating thickness increases with hydrophobic, electrostatically shielded tubes: Hair coating after dipping in dispersion of pristine (A), medium hydrophobic halloysite contact angle 84° and more hydrophobic halloysite contact angle 116° after 1 minute (B-C) and coating after 3-min treatment (D-F).

The coating of halloysite is more extensive with increasing degree of hydrophobicity of halloysite from pristine contact angle 14° to treated halloysite with 84° and finally 116° (Figure 5 A-C). After 3 minutes (longer) processing coating, the pictures follow the same trend with maximal coating over the entire hair surface with hydrophobic 116° halloysite (D-F). The higher hydrophobic halloysite displays the best (bulkier) self-assembly pointing to the fact that the coating on hair is dominated by Van der Waals forces.

2.2 Dye loading into halloysite tubes for colorant formulations.

Halloysite clay nanotubes have a 15 nm diameter lumen at the centre which is lined with alumina groups and the outer surface of the tubes is made up of coordinated silica molecules, providing inside / outside opposite charges at neutral pH [8,9]. This offers selectivity to negative compounds that can be loaded into the lumen. From cosmetic and therapeutic haircare formulations, we chose hair coloring as the first application for hair surface engineering. The dye selected was the anionic coloring molecule extracted from the henna plant (*Lawsonia inermis*): 2-hydroxy-1,4-naphthoquinone commonly known as lawsone.

Lawsone was loaded in halloysite lumen (Figure 6 F) by its dissolving in a mixture of water and acetone at saturated solubility of 45 mg ml^{-1} (Figure S6), followed by subjecting a mixture of halloysite and lawsone to overnight stirring and three short vacuum cycles of 30 min each. Lawsone is yellow in color in its non-dissociated form above pH 6, and it turns orange to brown in dissociated acidic form (below pH 3),[32] which is the desired shade for hair cosmetic care. However,

lawsone in solvents below pH 3 cannot bind to the keratin proteins on hair as they are negatively charged and unavailable for conjugating with the lawsone anion (1,2 quinone form).[32] Our choice of acetic acid to bring the pH down to 4.5 is significant as it aids in the swelling of hair. [33,34] Such hair swelling promotes initial anchoring of halloysite by creating more inter-cuticle spaces. Besides, acetic acid in the form of homemade vinegar has been traditionally used in human hair care.[35] We obtained selective 6.0 ± 1.0 wt. % lawsone loading into the halloysite lumen, leaving outer tube's surface intact for the self-assembly process. Such loaded and dried halloysite can be kept on shelf for years without any leakage of the dye to be used for hair coloring when needed.

With abovementioned (Results and Discussion, section 2.1) nanotube self-assembly procedure, we colored grey hair to red by 3 min washing with 0.75 wt. % dispersion of lawsone-loaded halloysite in acetic acid at pH 4.5. The color on the hair through the halloysite lumen lasted without change for six shampoo-water washing cycles (Figure 6). By themselves, halloysite nanotubes do not impart any color or opacity to the coating as is evidenced from various studies that underline the transparent property of halloysite in composite films [36–39]. Dark-field microscopy (Figure 6 D, E) was used in conjunction with hyperspectral imaging to demonstrate the changes in color induced by dye-loaded halloysite. From high resolution images (Figure 6 B-C), one can see that more intensive color is concentrated at the hair surface containing the layer of lawsone-halloysite.

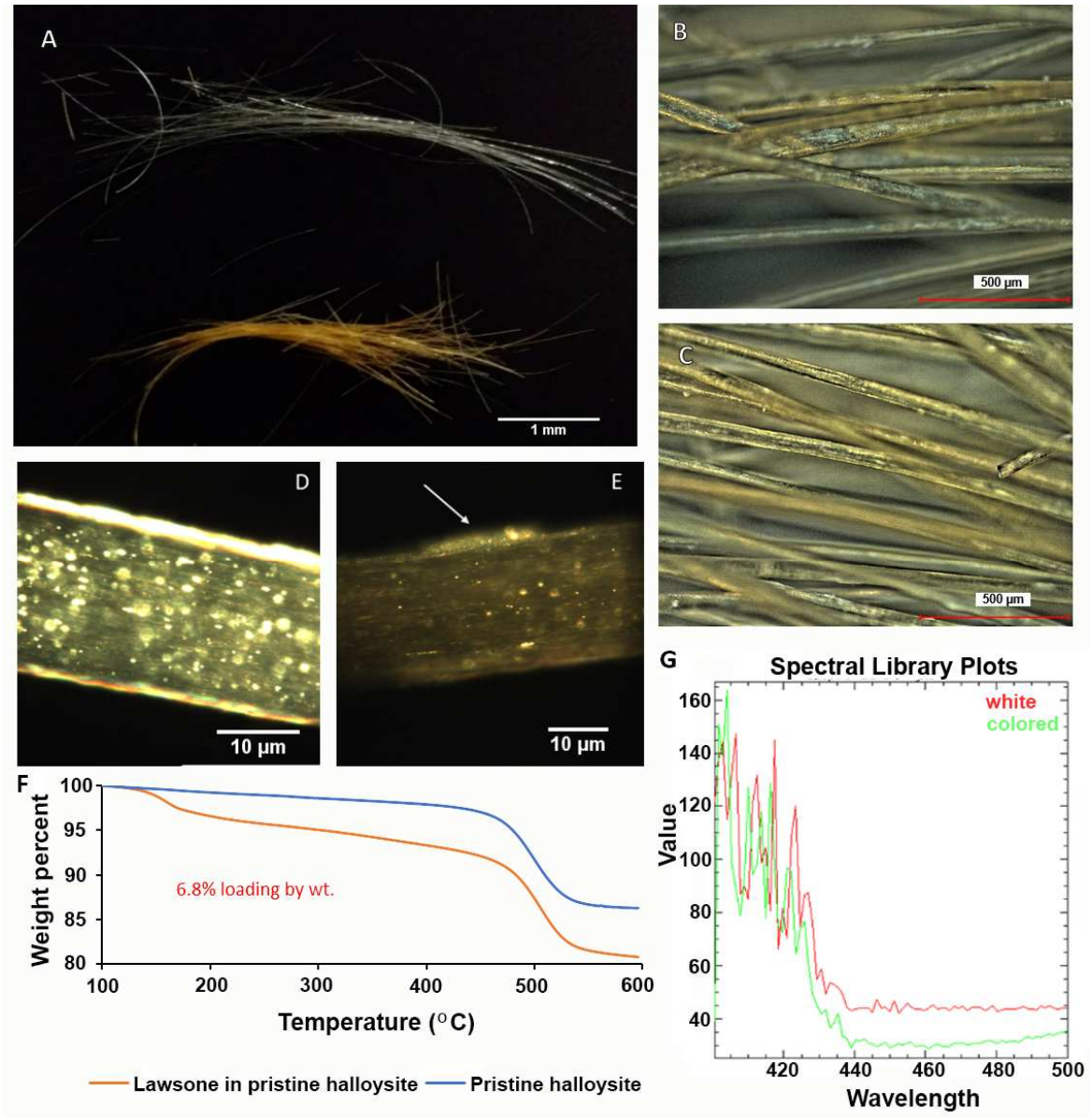

Figure 6: Color treatment of hair via halloysite self –assembly: Grey hair (upper image, A) washed for 3 minutes treated with an aqueous dispersion of lawsone-loaded halloysite gives bright orange color (bottom image, A). High definition images of hair coated with orange lawsone loaded halloysite (B-C). Dark field images of intact grey (D) and colored grey (E) hair from the same person (note the color change and the visible halloysite-dye aggregate indicated by arrow); reflected light spectra recorded in transmission dark field microscopy mode demonstrating the color change in grey hair after dye-halloysite composite deposition onto hair (G). The thermogravimetric analysis (TGA) results of lawsone-loaded halloysite tubes (F) shows their increased weight loss against pristine halloysites referring to the incineration of organic dye content.

We have to underline that the described procedure is applicable for any dyes, including non-water soluble ones which may be loaded into hydrophobized halloysite lumens.[15,16] Color molecules blue indigo carmine, shikonin, carmine from the *Indigofera tinctifera*, *Alkanna tinctoria* plants and

Dactylopius coccus insect can be loaded inside the nanotube lumen, keeping the formulation natural preventing allergic reactions.[40,41] Our formulation for hair coloring avoids direct contact of dyes to hair, replacing the currently accepted hair chemical modification process to the physical sorption self-assembly. This approach may drastically widen the color palette for the hair care with the clay encapsulation of dyes which, for different reasons, are prevented from use in human haircare products. Apart from human hair, the robust drug-loaded halloysite assembly was successfully realized on different animals' hair: dog, cat and horse (Figures S9-S11).

2.3 Drug loading into halloysite nanotubes for sustained medical treatment

Hair can not only be affected from age discoloration or other cosmetic defects, but also be infected by insects, fungi and other micro-organisms. Halloysite self-assembly on hair can act as potent treatment to reduce the therapeutic burden of such problems by loading the lumen with active pharmaceutical molecules with sustained delivery over few days.

Lice infestations carry an uneasy past with prevalent growth and spread and continue to be a menace, especially in young children and farm animals. The human lice, *Pediculus humanus capitis*, spend their lifespan on the hair, resting and laying eggs from near the scalp.[42] Popular anti-lice treatments, containing pyrethroids, are available as scalp creams and shampoos.[43,44] Over the recent years, these drugs are losing efficacy as lice are developing resistance against the active agents, besides it is easily washed out and have to re-applied periodically.[7] Non-availability of the active drug at the primary target site into the cuticles is one of the reasons for the resistance.[42,44] Halloysite, with their robust assembly on the hair surface and ability to carry load of drugs within its lumen, can target the hair cuticle gaps which are the primary site of infestations and propagation for the lice.

Permethrin, a widely used synthetic pyrethroid, is a water-insoluble potent anti-lice compound.[28,43] To encapsulate it in halloysite, the nanotube's lumen was hydrophobized to enhance loading with hydrophobic permethrin. Another chosen hair drug was minoxidil, which has been proven to induce hair growth factors topically and is prescribed as an effective medication against alopecia. [45–49]

We performed a hydrophobic modification of halloysite lumens done by selective absorption of negative surfactant, sodium dodecyl sulfate (SDS) into positive lumen. Twelve carbon atoms aliphatic chain provides the necessary hydrophobicity to the inner surface of the nanotubes allowing for loading water-insoluble active compounds from their respective organic solutions (Figure 7A), which is confirmed by increase of the halloysite ζ-potential from -30 to -62 mV due to neutralization of the inner cation groups (Figure S8). TGA analysis indicated 3.0 ± 0.1 wt. % permethrin and 6.9 ± 0.1 wt. % minoxidil contents and such loaded nanotubes may be kept without loss of drug for a long time and applied as assembled layer onto hair after simple washing with halloysite dispersion (Figure 7 B, C respectively).

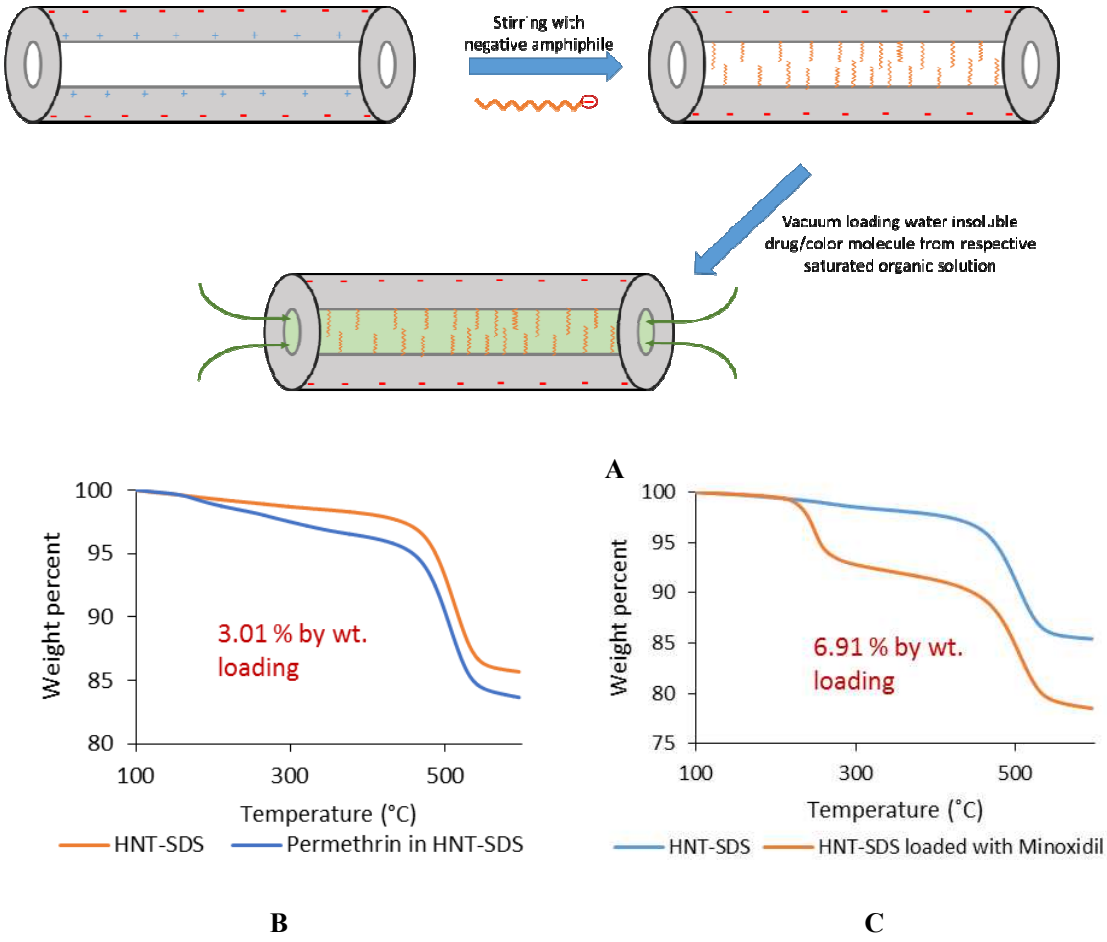

Figure 7. Illustration of SDS-amphiphile coating inside lumen aiding in loading water insoluble compounds (permethrin and minoxidil) into halloysite lumen (A). TGA spectra of halloysites pre-treated with SDS and loaded with water insoluble active agents, permethrin (B) and minoxidil (C).

After loading, the drugs were slow released from the clay nanotubes during 2-3 days which will allow for a sustained hair treatment.

2.4 Biocide efficiency of the drug-loaded halloysite

As a proof of concept of drug-loaded halloysite for anti-lice treatment, we employed *Caenorhabditis elegans* nematodes to investigate the *in vivo* uptake and toxic effects of permethrin-halloysite formulations. Loading of biocidal drugs, such as permethrin, into halloysite followed by an application on hair will be an excellent approach to pediculosis and scabies which are caused by arthropod ectoparasites.[50] Nematodes belong to a different invertebrate type than arthropods, but they have been reported to be susceptible to permethrin.[51] Using nematodes in permethrin-halloysite toxicity testing allows avoiding the drawbacks of lice infestation in humans.[52] We followed our previously published protocol[11] using wild type *C. elegans* which were subjected to 250 μm ml^{-1} permethrin- halloysite. The permethrin-loaded nanotubes adhered to the nematode cuticle (Figure 8 a-b), and we also detected nanotubes in their intestines. We detected the increased number of dead animals having rod-shaped rigid appearance (Figure 8 c) and having abnormal morphologies (Figure 8 d). After 24 h of co-incubation of young adult (L4 growth stage) *C. elegans* nematodes with permethrin-halloysite, 85% of worms were dead, as detected by lack of touch-induced movement. We have previously shown that pristine halloysite does not induce any toxicity in C. elegans, even at high concentration and prolonged exposure [11] and thus the mortality of worms was only due to the effect of permethrin release from the tubes' lumen. The worms investigated in this study were exposed to halloysite loaded with permethrin, therefore the animals took up the nanotubes-loaded drug. Our results suggest that halloysite loaded with permethrin facilitates the biocide effect of permethrin, apparently due to the increased uptake during halloysite penetration in intestines.

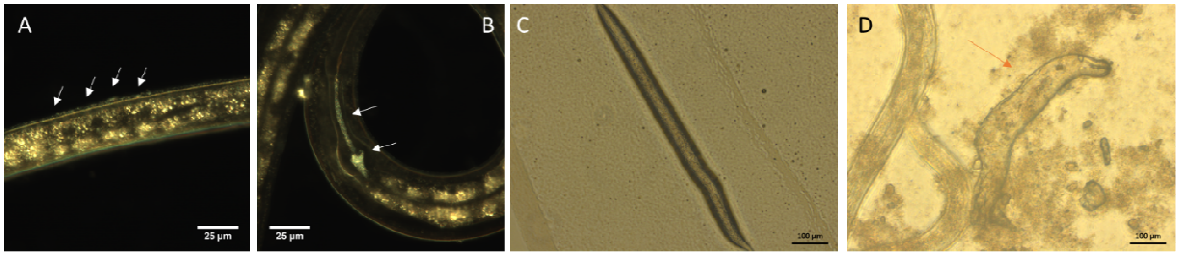

Figure 8. Permethrin-loaded halloysite was detected both on cuticle (A) and in intestines (B) of C. elegans nematodes killing the worms (C) and inducing the abnormal morphologies (D).

We have used *C. elegans* as a convenient model to demonstrate the toxicity of permethrin loaded into halloysite lumens. In our future work we expect to perform to extend our investigation of the effects of this material on lice. Since halloysite effectively forms uniform layered coatings on hair surface, insecticide-loaded nanotubes assembled onto human or animal hair would bring the drug into the direct contact with lice, which normally move along the hair and firmly attach their eggs and nits to hair surface.[53] In case of halloysite-based insecticide use, the parasites will be exposed to the high-density drug-filled coating, thus increasing the efficacy and duration of the treatment, enabling extended exposure for treatment. Our future experiment will include quantifying lice-killing effects of insecticide-loaded clay nanotubes according to established veterinary protocols and may even require experiments involving human volunteers.

3. Experimental section

Halloysite clay nanotubes were obtained from Applied Minerals, Inc. with origin at Dragon mine, Utah, USA. Human hair samples were procured from a healthy Caucasian female, 20 years old with no special treatment. Grey hairs were obtained from 56 y.o. male. Samples were procured from all human subjects with informed consent. Non-treated hair possesses all the usual layers on the cuticle, including the 18-methyl eicosanoic acid (18-MEA) lipid layer, which is crucial to study behaviour of normal hair. Sodium dodecyl sulfate, lawsone, minoxidil and permethrin were purchased from Sigma-Aldrich.

Halloysite clay nanotubes, which have been milled and washed, were dispersed with deionized water. The clay concentration was optimised at 7.5 mg ml^{-1} (Table S2, Figure S6). 4-5 cm hair

strands were rinsed in the dispersion for 1-5 minutes (optimum 3 min), further washed with pure warm water and dried. This method was used for all coating procedures, including hydrophobic and loaded halloysite.

3.1 Sample imaging

A Hitachi FE SEM was used for the image procurement. For scanning electron microscopy - SEM, hair samples were cut into 1-2 mm pieces with a slant edge of a razor blade. The slant cuts of the hair make the cross-section more visible, giving a perspective to the hair surface being analysed. 1-2 strands about 5 cm long are cut into such pieces which are then placed on top of a carbon adhesive tape through a small plastic cone to form a heap. The small heap of hair fragments on the tape is subjected to a gold coating (Cressington 208HR sputter coater) of 4 nm for better resolution under the electron beam.

3.2 Transmission Electron Microscopy (TEM) and Scanning Electron Microscopy (SEM)

Images were obtained at the Shared Instrumentation Facility of Louisiana State University (Baton Rouge, LA) using a JEOL 1400 Biological and Soft Material TEM where the strands of hair sample were embedded into an epoxy resin to be cut into cross and longitudinal sections. Regular fixatives and buffer washes before the embedding were avoided to leave the coating on hair unchanged. For SEM imaging and EDX analysis dry hair samples (intact and halloysite-coated) were sputtered with a thin gold layer using a BalTec sputter coater. Images were obtained using an Auriga SEM operated at 20 kV accelerating voltage. SEM images were obtained for top view and profile view of the freshly cut hair.

3.3 Profilometry and confocal microscopy

3-D profilometer and confocal Keyence VK-X150 microscope was used; sample preparation and image processing: 500X and 1000 X magnification (50X and 100X objective lenses) of a microscope were employed to view the hair, with the 1000X magnification used for better detail. The hair samples are perched on top a glass slide under enough tension to keep it straight with the

help of adhesive tapes. After collecting the laser and optical images, the images are processed for noise reduction, Dark and Bright clearance, height cut-off and tilt correction before the roughness analysis. Accounting the irregular curvature of hair surface, the tilt of the surface was corrected to a near perfect semi-circular profile. The area to be analyzed was fixed to a rectangle of 75 x 25 μm measured at the centre of the extracted surface with minimum curvature possible. The roughness parameter considered is Rq which is the root mean square of all measurements in the considered rectangle area.

3.4 Atomic Force Microscopy

Dimension FastScan instrument (Bruker) operated by using Bruker Nanoscope software in ScanAsyst™ mode in air using silicon-nitride ScanAsyst Air probes (nominal tip radius 2 nm) was used to visualise halloysite tubes.

3.5 Dye and drug loading into halloysite

Lawsone was checked for maximum solubility in differing ratios of water and acetone and excess of acetone at 1:8 by volume respectively was found to be optimum (Figure S6-A). Halloysites both pristine and with a hydrophobic lumen were dispersed in 45 mg ml^{-1} solution of lawsone in the water-acetone mixture. The dispersion was sonicated for 5 min in order to break apart any halloysite aggregates and expose individual tubes' lumen to loading. After stirring for 5 hours, the mixture is subject to vacuum for 30 min. The solvent is replenished after the vacuum time and mixture is again stirred for 1 hour. Sonication at this stage is forbidden as it would cause the load of lawsone to release immediately from the lumen. The vacuum and stirring cycle is repeated for 2 more times followed by drying under vacuum. The dried halloysites are washed with the solvent and centrifuged at 5000 rpm for 2 min to remove the excess lawsone. The final loaded tubes are kept under vacuum overnight to dry out.

3.6 Hydrophobization of the nanotube lumen

Halloysite nanotubes were dispersed thoroughly through sonication in a solution of SDS at 2 mg ml^{-1} with the weight ratio of halloysite: SDS being 1:1. Below the critical micellar concentration,

SDS is in solution as linear chains and hence more probably to enter the 15 nm wide lumen of halloysite tubes. SDS have been previously to modify lumen with a different protocol by Cavallaro et al[16]. The halloysite-SDS dispersion is allowed to stir for 48 hours followed by centrifugation for 3 min at 1000 rpm. The absorption of SDS on positive alumina groups neutralize the positive charges and increases the net negative charge of halloysite tubes (ζ-potential measured with Brookhaven ZetaPlus Instrument) imparting greater ability to remain in dispersion. Tubes that are successfully modified (halloysite-SDS) tend to remain as colloid, and the centrifugation helps to select such halloysites from supernatant and eliminate the pellet of non-modified tubes. The selected supernatant is centrifuged at a higher speed and time of 5000 rpm, 20 min to separate out the halloysite-SDS. The separated halloysite are subjected to series of washes with DI water to remove the excess surfactant until the washings possess the same surface tension as water. The surface tension was measured using a pendant drop goniometer. After the washings, which were normally 4-5, the halloysites were dried overnight under vacuum. The product was tested for zeta potential and loading by TGA. Thermogravimetry (TGA) was performed with a Thermal Advantage Q50 instrument. UV–vis analysis was performed using an Agilent spectrophotometer.

3.7 Loading permethrin and minoxidil inside halloysite-SDS lumen

Permethrin is dissolved in acetone at 20 mg ml^{-1} and halloysite-SDS are dispersed in the solution at the same concentration. Halloysite-SDS and minoxidil are added to methanol at 50 mg ml^{-1} each and dispersed through sonication. The respective dispersions are stirred overnight and then subject to vacuum and stirring cycles for 30 min and 1 hour respectively three times. The solvents are replenished after every vacuum step. The solvent is dried off under vacuum after the third cycle and the dried tubes are washed with their respective solvents and centrifuged at 5000 rpm for 2 min to separate out the excess drugs in both cases. The washed product is dried under vacuum and analysed for loading with TGA (for more illustration, see Figure 7A).

3.8 *C. elegans* worms' maintenance and toxicity testing: *Caenorhabditis elegans* wild type strain (N2 Bristol) was maintained at 20°C in darkness on agar-based nematode growth medium (NGM)

(US Biological, USA) plastic plates with Escherichia coli OP50 bacteria as a food source. To obtain the synchronized worms, the gravid adults were washed from the dishes with M9 buffer (22 mM KH_2PO_4, 42 mM Na_2HPO_4, 85.5 mM NaCl, 1 mM $MgSO_4$), centrifuged and then the pellet was mixed with aqueous 2 % NaOCl and 0.45 M NaOH and incubated for 10 min. After the complete decomposition of all live worms the preserved eggs were washed with M9 buffer several times and transferred to new sterile NGM plates. After 24 hours of incubation at 20 °C, the plates were filled with permethrin-loaded halloysite nanotubes or pristine halloysite as control samples. Routine observation of nematodes was performed using a Nikon SMZ 745 T stereomicroscope. Dark field (DF) microscopy images of halloysite distribution on nematode cuticle and in intestines were obtained using a CytoViva® enhanced dark-field condenser attached to an Olympus BX51 upright microscope equipped with 100x fluorite objective (variable numerical aperture 0.6 – 1.3), ProScan III (Prior) scanning module and DAGE CCD cooled digital camera. Fiber-Lite DC-950 (Dolan-Jener) with 150W quartz halogen bulb was used for illumination. Images were captured using Exponent 7 imaging software (Dage-MTI). For reflected light spectra collection, the samples were illuminated in dark-field mode. The spectral libraries were collected using a Specim V10E spectrometer and PCO.PixelFly CCD camera. Spectra were collected in 400 – 1000 nm region, spectral resolution was 2 nm using ENVI 4.8 software (Harris Geospatial Solutions). Extra clean dust-free Nexterion® glass slides and coverslips (Schott, Germany) were used for dark field microscopy imaging to minimize dust interference. For SEM imaging and EDX analysis dry hair samples (intact and halloysite-coated) were sputtered with a thin gold layer using a BalTec sputter coater. Images were obtained using an Auriga SEM operated at 20 kV accelerating voltage. SEM images were obtained for top view and profile view of the freshly cut hair.

4. Conclusion

Hair is an important protective coating in mammals; for humans, it also plays a crucial role as a part of personality and mental well-being. Here we have introduced a facile and robust hair surface engineering scheme to immobilize pristine and chemically-modified clay nanotubes onto hair

cuticles. Self-assembly of halloysite clay occurs within few minutes and results in formation of a dense 3-5 μm layer of the nanotubes on hair surface, significantly altering its optical and structural properties. The surface modification of hair with clay nanotubes is very resilient, withstanding up to 10 shampoo washes. The method is universal and works well with both human and animal hair, as tested with dog, cat and horse hair.

Importantly, halloysite nanotubes, a natural biocompatible material having 10-20 % loading capacity due to its lumen, with the ability to encapsulate functional molecules (dyes or drugs), render the hair surface with novel functionalities. We demonstrated the application of dye-loaded halloysite nanotubes as a novel replacement for conventional hair coloring. Halloysite-based hair dye treatment was effective for coloring of both pigmented and grey hair.

We also report a novel approach for topical drug administration using hair surface coating with the nanoclay. Halloysite can be loaded with a wide selection of drugs (e.g., minoxidil), sustaining their gradual slow release; therefore, the assembly of such loaded nanotubes on hair will facilitate the delivery of drugs. As a proof-of-concept, we loaded the insecticide permethrin into halloysite lumens and assembled the drug-loaded nanotubes on hair. Permethrin-loaded halloysite was effective against *C. elegans* nematodes, suggesting that a similar effect will be demonstrated in practical purposes for lice and scabies elimination. This approach to tailor clay nanocontainers loaded with anti-parasite treatments might find application in treating lice infestations in humans and also in animals.

5. Acknowledgements

AP and YL thank NSF grant #1547693 and Louisiana Biomedical Research Foundation for partial support. Any opinions, findings, and conclusions or recommendations expressed in this report are those of authors and do not necessarily reflect the view of National Science Foundation. The work was performed by RF and GF according to the Russian Government Program of Competitive Growth of Kazan Federal University and by the subsidy allocated to Kazan Federal University for the state assignment in scientific activities, #16.2822.2017/4.6 and by RFBR grant #18-29-11031. The authors

thank Mark DeCoster (LaTech), Evgeniy Nuzhdin and Daut Bakeev (Kazan University) for useful discussion and help with scanning electron microscopy. Scheme 1A artwork courtesy: Nick Bustamante.

6. Conflict of Interest

The authors declare no conflict of interest.

7. References

1 C. Bolduc and J. Shapiro, *Clin. Dermatol.*, 2001, **19**, 431–436.

2 C. R. Robbins, in *Chemical and Physical Behavior of Human Hair*, Springer Berlin Heidelberg, Berlin, Heidelberg, 2012, pp. 1–104.

3 G. Nohynek, R. Fautz, F. Benech-Kieffer and H. Toutain, *Food Chem.*, 2004, **42**, 517–543.

4 C. R. Robbins, in *Chemical and Physical Behavior of Human Hair*, Springer Berlin Heidelberg, Berlin, Heidelberg, 2012, pp. 263–328.

5 C. R. Robbins, in *Chemical and Physical Behavior of Human Hair*, Springer Berlin Heidelberg, Berlin, Heidelberg, 2012, pp. 329–443.

6 H. J. Ahn and W. S. Lee, *Int. J. Dermatol.*, 2002, **41**, 88–92.

7 M. Semmler, F. Abdel-Ghaffar, S. Al-Quraishy, K. A. S. Al-Rasheid and H. Mehlhorn, *Parasitol. Res.*, 2012, **110**, 273–276.

8 Y. Lvov, W. Wang, L. Zhang and R. Fakhrullin, *Adv. Mater.*, 2016, **28**, 1227–1250.

9 M. Liu, Z. Jia, D. Jia and C. Zhou, *Prog. Polym. Sci.*, 2014, **39**, 1498–1525.

10 Y. M. Lvov, M. M. DeVilliers and R. F. Fakhrullin, *Expert Opin. Drug Deliv.*, 2016, **13**, 977–986.

11 G. I. Fakhrullina, F. S. Akhatova, Y. M. Lvov and R. F. Fakhrullin, *Environ. Sci. Nano*, 2015, **2**, 54–59.

12 M. Makaremi, P. Pasbakhsh, G. Cavallaro, G. Lazzara, Y. K. Aw, S. M. Lee and S. Milioto, *ACS Appl. Mater. Interfaces*, 2017, **9**, 17476–17488.

13 E. Abdullayev, A. Joshi, W. Wei, Y. Zhao and Y. Lvov, *ACS Nano*, 2012, **6**, 7216–7226.

14 E. Abdullayev, R. Price, D. Shchukin and Y. Lvov, *ACS Appl. Mater. Interfaces*, 2009, **1**,

1437–1443.

15 G. Cavallaro, G. Lazzara and S. Milioto, *J. Phys. Chem. C*, 2012, **116**, 21932–21938.

16 G. Cavallaro, G. Lazzara, S. Milioto, F. Parisi and V. Sanzillo, *ACS Appl. Mater. Interfaces*, 2014, **6**, 606–612.

17 V. A. Vinokurov, A. V. Stavitskaya, E. V. Ivanov, P. A. Gushchin, D. V. Kozlov, A. Y. Kurenkova, P. A. Kolinko, E. A. Kozlova and Y. M. Lvov, *ACS Sustain. Chem. Eng.*, 2017, **5**, 11316–11323.

18 E. Abdullayev and Y. Lvov, *J. Mater. Chem.*, 2010, **20**, 6681.

19 J. Tully, R. Yendluri and Y. Lvov, *Biomacromolecules*, 2016, **17**, 615–621.

20 N. G. Veerabadran and R. R. Price, *NANO Br. Reports Rev.*, 2007, **2**, 115–120.

21 E. Abdullayev and Y. Lvov, *J. Nanosci. Nanotechnol.*, 2011, **11**, 10007–10026.

22 Y. Zhao, G. Cavallaro and Y. Lvov, *J. Colloid Interface Sci.*, 2015, **440**, 68–77.

23 G. Cavallaro, G. Lazzara, S. Milioto, F. Parisi and V. Sanzillo, *ACS Appl. Mater. Interfaces*, 2014, **6**, 606–12.

24 G. Lazzara, G. Cavallaro, A. Panchal, R. Fakhrullin, A. Stavitskaya, V. Vinokurov and Y. Lvov, *Curr. Opin. Colloid Interface Sci.*, 2018, **35**, 42–50.

25 M. Liu, Z. Huo, T. Liu, Y. Shen, R. He and C. Zhou, *Langmuir*, 2017, **33**, 3088–3098.

26 G. M. Whitesides, *Science (80-.).*, 2002, **295**, 2418–2421.

27 D. Taplin, T. L. Meinking, S. L. Porcelain, P. M. Castillero and J. A. Chen, *J. Am. Acad. Dermatol.*, 1986, **15**, 995–1001.

28 D. Taplin, T. L. Meinking, P. M. Castiliero and R. Sanchez, *Pediatr. Dermatol.*, 1986, **3**, 344–348.

29 B. S. Richard A. Lodge, in *Climate Change 2013 - The Physical Science Basis*, ed. Intergovernmental Panel on Climate Change, Cambridge University Press, Cambridge, 2007, pp. 1–30.

30 R. A. Lodge and B. Bhushan, *J. Appl. Polym. Sci.*, 2006, **102**, 5255–5265.

31 C. Popescu and H. Höcker, *Chem. Soc. Rev.*, 2007, **36**, 1282–1291.

32 B. I. H. Amro, K. C. James and T. D. Turner, *J. Soc. Cosmet. Chem.*, 1994, **165**, 159–165.

33 E. Valko and G. Barnett, *J. Soc. Cosmet. Chem.*, 1952, **3**, 108–117.

34 US Patent Office, US 5474578 A, 1995.

35 J. Galvin and D. Galvin, in *Hair Matters*, Macmillan Education UK, London, 1985, pp. 21–29.

36 G. Cavallaro, D. I. Donato, G. Lazzara and S. Milioto, *J. Phys. Chem. C*, 2011, **115**, 20491–20498.

37 C. S. Yelleswarapu, G. Gu, E. Abdullayev, Y. Lvov and D. V. G. L. N. Rao, *Opt. Commun.*, 2010, **283**, 438–441.

38 K. Prashantha, M.-F. Lacrampe and P. Krawczak, *J. Appl. Polym. Sci.*, 2013, **130**, 313–321.

39 K. Fujii, A. N. Nakagaito, H. Takagi and D. Yonekura, *Compos. Interfaces*, 2014, **21**, 319–327.

40 S. Komboonchoo and T. Bechtold, *J. Clean. Prod.*, 2009, **17**, 1487–1493.

41 H. C. Wang and C. Y. Chen, *Sen-I Gakkaishi*, 2009, **65**, 276–281.

42 C. G. Burkhart and C. N. Burkhart, *Expert Opin. Drug Saf.*, 2006, **5**, 169–79.

43 C. Cummings, J. Finlay and N. Macdonald, *Paediatr Child Heal.*, 2014, **13**, 692–6.

44 C. N. Burkhart and C. G. Burkhart, *Int. Pediatr.*, 2002, **17**, 209–212.

45 J. S. Storer, J. Brzuskiewicz, H. Floyd and J. C. Rice, *Am. J. Med. Sci.*, 1986, **291**, 328–333.

46 S. Lachgar, M. Charveron, Y. Gall and J. L. Bonafe, *Br. J. Dermatol.*, 1998, **138**, 407–411.

47 A. W. Lucky, D. J. Piacquadio, C. M. Ditre, F. Dunlap, I. Kantor, A. G. Pandya, R. C. Savin, M. D. Tharp and B. E. Kohut, *J. Am. Acad. Dermatol.*, 2004, **50**, 541–553.

48 A. E. Buhl, D. J. Waldon, C. A. Baker and G. A. Johnson, *J. Invest. Dermatol.*, 1990, **95**, 553–557.

49 A. G. Messenger and J. Rundegren, *Br. J. Dermatol.*, 2004, 150, 186–194.

50 K. Gunnung, K. Pippitt, B. Kiraly and S. Morgan, *Am. Fmily Physician*, 2013, **24**, 211–216.

51 F. Boufahja, B. Sellami, M. Dellali, P. Aïssa, E. Mahmoudi and H. Beyrem, *Nematology*, 2011, **13**, 901–909.

52 I. F. Burgess, E. R. Brunton and N. A. Burgess, *BMC Dermatol.*, 2013, **13**, 5.

53 H. Lapeere, L. Brochez, E. Verhaeghe, R. H. Vander Stichele, J.-P. Remon, J. Lambert and L. Leybaert, *J. Med. Entomol.*, 2014, **51**, 400–407.

Keyword

Halloysite clay nanotubes; hair formulation; hair color; self-assembly; anti-lice

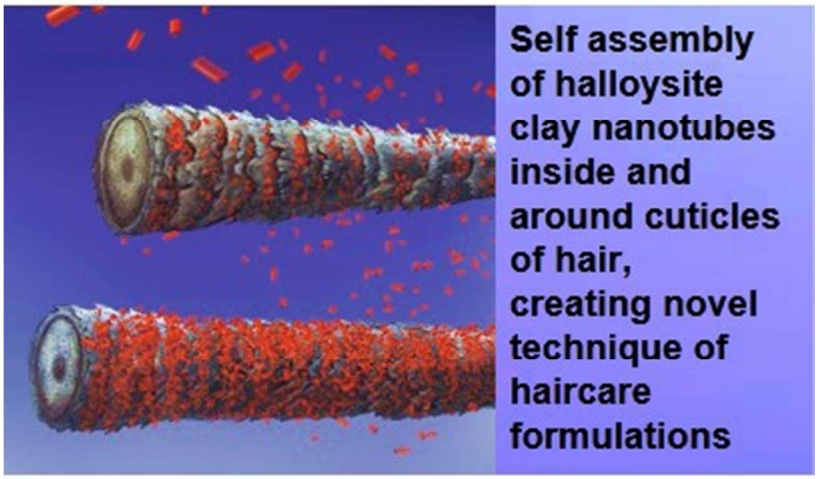

68x40mm (150 x 150 DPI)